

High-Throughput Design of Refractory High-Entropy Alloys: Critical Assessment of Empirical Criteria and Proposal of Novel Guidelines for Prediction of Solid Solution Stability

Giovanni Carlucci, Cristina Motta, and Riccardo Casati*

Refractory high-entropy alloys (RHEAs) are a new class of metallic alloys which have been extensively studied in the past decade due to their excellent high-temperature performances. However, the design of new lightweight and ductile RHEAs is a challenging task, since an extensive exploration of the immense compositional space of multicomponent systems is practically impossible.

Aiming to reduce the experimental effort, several research groups have proposed different predictive criteria to design new high-performing HEAs. Nevertheless, the criteria proposed so far are often based on a limited amount of data and, generally, do not differentiate between refractory and nonrefractory HEAs. To overcome these limitations, herein, a comprehensive database of properties of 265 RHEAs reported in the open literature from 2010 to 2022 is developed. Such a database is used to assess the validity of predictive empirical criteria and new guidelines for the prediction of solid solution stability in RHEAs are proposed.

on microstructural features and mechanical properties of metallic materials. As a rule of thumb, when the concentration of solute elements is rather low, the microstructure of alloys assumes the characteristics of a solid solution (SS) that is usually characterized by a ductile behavior.^[2] At higher concentrations, alloying elements tend to form intermetallic (IM) compounds, commonly leading to low ductility and high strength. This explains why the chemical composition range of metallic alloys is usually limited to the corners of phase diagrams, where one element dominates on the others.^[3]

In 2004, Yeh, Cantor, and respective co-workers^[4,5] independently proposed a new strategy to design metallic alloys. They were able to stabilize in alloys single-phase SS by increasing the concentration of the alloying elements, in order to reach an equiatomic mixing. The term “high-entropy alloys” (HEAs) was therefore coined to denominate this new class of alloys, generally composed by more than five principal elements.

The key concept behind the stability of a phase with respect to another is the minimization of the Gibbs free energy of the desired phase, that is

$$\Delta G = \Delta H - T\Delta S \quad (1)$$

Therefore, the stability of the SS with respect to IMs in HEAs was justified by Yeh et al. by the increase of the configurational entropy of the mixture (ΔS_{mix}) due to the high concentrations of alloying elements.^[4] Indeed, high ΔS_{mix} values reduce the Gibbs free energy of mixing (ΔG_{mix}) to values lower than the Gibbs free energy of formation of IM compounds (ΔG_{IM}), thus stabilizing the SS.

HEAs have attracted great interest from the research community in the past two decades^[1–3,6] since numerous HEAs showed superior mechanical and physical properties with respect to conventional metallic alloys, such as outstanding toughness at cryogenic temperature,^[7] increased thermal stability on a wide temperature range,^[8,9] and the overcoming of the strength–ductility trade-off.^[10]


Regarding alloys for high-temperature applications, Senkov et al. pioneered the field of refractory high-entropy alloys (RHEAs) with their studies on MoNbTaW and MoNbTaVW

1. Introduction

Metallic alloys are conventionally designed in terms of a solvent–solute criterion:^[1] the base element—which is present in high concentrations and determines the main properties of the alloy—is considered a solvent, whilst the other alloying elements—which are added in minor concentrations—act as solutes. The advantage related to this approach is the possibility to tune the properties of the base material by controlling its chemical composition.

Indeed, the concentration of solute elements, as well as the processing and postprocessing conditions, have great influence

G. Carlucci, C. Motta, R. Casati
Department of Mechanical Engineering
Politecnico di Milano
Via La Masa 1, 20156 Milano, Italy
E-mail: riccardo.casati@polimi.it

 The ORCID identification number(s) for the author(s) of this article can be found under <https://doi.org/10.1002/adem.202301425>.

© 2023 The Authors. Advanced Engineering Materials published by Wiley-VCH GmbH. This is an open access article under the terms of the Creative Commons Attribution-NonCommercial-NoDerivs License, which permits use and distribution in any medium, provided the original work is properly cited, the use is non-commercial and no modifications or adaptations are made.

DOI: 10.1002/adem.202301425

equiatomic alloys.^[8,9] The alloys which belong to this class of HEAs are based on elements of the IV, V, and VI groups, that is, Ti, V, Cr, Zr, Nb, Mo, Hf, Ta, W. Though RHEAs exhibit unprecedented combination of properties, they also show some shortcomings that need to be faced. Many RHEAs show indeed density higher than 12 g cm^{-3} , low ductility at room temperature, and contain expensive elements, compromising the industrial uptake.^[6]

A common strategy that has been investigated to decrease the density of RHEAs consists of the replacement of heavy refractory elements—such as W, Ta, Hf—with lighter refractory elements—such as Ti, Zr, and V.^[11,12] Moreover, the density of RHEAs can be further decreased by adding light nonrefractory elements, such as aluminum,^[13,14] to a certain extent. However, due to the negative enthalpy of mixing between aluminum and many refractory elements, brittle IMs are likely to form.^[2]

The design of HEAs is a challenging task, especially when dealing with nonequiatomic compositions, since the unexplored regions of the phase diagrams of these multicomponent systems are immense.^[1,3] To reduce the experimental effort, several methods to predict the formation of SSs have been proposed, which can be divided into two main groups, namely empirical and computational methods. The empirical methods are based on the Hume–Rothery rules and several thermodynamic parameters.^[15,16] The computational methods rely on CALPHAD calculations,^[17,18] atomistic simulations,^[19,20] and machine learning algorithms.^[21,22] The present study focuses on predictive methods based on empirical parameters.

As demonstrated by Otto et al.,^[23] ΔS_{mix} appears not able to precisely predict the stability of SS even in equiatomic HEAs. Therefore, in the past years, different empirical parameters have been proposed in order to foresee phase stability and mechanical properties of HEAs.^[3,15] According to the Hume–Rothery rules,^[2] composition-weighted parameters such as the enthalpy of mixing, the atomic size mismatch, the electronegativity difference, and the average valence electron concentration (VEC) have been evaluated.^[24–28]

The predicting empirical criteria proposed so far have been often assessed by relying on a limited amount of data. Moreover, most of such criteria are based on data that refer to alloys in the as-cast condition, which can be misleading. Indeed, an as-solidified microstructure is generally heterogeneous and usually SSs are stabilized by quenching HEAs from high temperatures.^[29] Moreover, usually the datasets do not differentiate between refractory and nonrefractory HEAs, which are commonly characterized by a body-centered cubic (BCC) and a face-centered cubic (FCC) structure, respectively.^[15]

Given this context, we developed a wide database including the properties of 265 RHEAs that have been developed and reported in the open literature so far. The validity of predictive empirical criteria proposed in the literature have been assessed using the data collected in the database. Moreover, the collected data has been used to investigate on the relationship between empirical parameters and microstructure and mechanical properties of RHEAs and to propose new criteria that are more robust than those proposed so far because based on much larger number of alloy properties. Such guidelines will be a useful high-throughput tool that will be available to material designers for the development of new RHEAs.

2. Database

The database has been developed by an in-depth literature review on RHEAs. The data have been extracted from the first paper of Senkov and colleagues that was published in 2010^[9] to a work of Wang et al.^[30] published in 2022. For each alloy, the database includes the following information: chemical composition, alloy density, measured or calculated melting temperature, stable phases (SS and/or IM), empirical parameters, and mechanical properties.

More in the detail, the database includes the following parameters that were calculated based on the chemical composition of RHEAs: average VEC, atomic size mismatch (δr), electronegativity difference ($\delta \chi$), enthalpy of mixing (ΔH_{mix}), entropy of mixing (ΔS_{mix}), enthalpy of formation of IM compounds (ΔH_{IM}), excess entropy (S_{XS}), and the Ω , Λ , Φ , κ_1 , and κ_1^{c} parameters. More details about the different parameters used in this study and equations for their calculations will be provided in the following paragraphs. The mechanical properties include the yield stress (σ_y), the peak stress (σ_p), the specific yield or peak stress (σ/ρ , where ρ is the density of the alloy), the strain at failure (ϵ_f), and the elastic modulus (E). Moreover, for each mechanical property, it has been reported whether it refers to compression or tension tests, the testing temperature, the strain rate, and the testing condition of the material, for example, as cast or annealed.

The database totally collects 265 RHEAs with different compositions, belonging to 111 different alloy systems. Among the collected alloys, 104 have been tested in the annealed condition and, among them, only eight have been tested in tension. For the purposes of this work, due to the limited amount of data related to tensile properties, we focused the analysis on annealed RHEAs tested in compression at room temperature (in total, 96 alloys).^[9,11,13,14,31–62]

3. Review of Empirical Criteria for Prediction of Phase Stability

The first models that have been proposed were mainly based on the Hume–Rothery rules, which state that the combination of elements with similar atomic size, crystal structure, electronegativity, and valence leads to a higher likelihood to form SSs.^[2]

The effect of the atomic size is significant because it strictly influences lattice distortion, sluggish diffusion, and phase stability.^[63] The Hume–Rothery rule for atomic radius mismatch for conventional alloys consists of the comparison of the size of the principal element atoms with that of the other alloying elements. In the case of HEAs, the distinction between solute and solvent atoms loses its meaning, and each element has the same probability to occupy a lattice site.^[24,63,64] Therefore, it is more convenient to use a statistical approach to calculate the atomic size mismatch, that is, the standard deviation between the radii of all the components.

$$\delta r = \sqrt{\sum_i x_i \left(1 - \frac{r_i}{\bar{r}}\right)^2} \quad (2)$$

where r_i and x_i are the atomic radius and the atomic fraction of the i -th element, respectively, and $\bar{r} = \sum x_i r_i$. An analogous approach can be used to calculate the electronegativity difference.

$$\delta\chi = \sqrt{\sum_i x_i \left(1 - \frac{\chi_i}{\bar{\chi}}\right)^2} \quad (3)$$

where χ_i is the electronegativity of the i -th element, and $\bar{\chi} = \sum x_i \chi_i$.

The enthalpy of mixing and the entropy of mixing are calculated as

$$\Delta H_{\text{mix}} = \sum_{i < j} 4H_{ij}x_i x_j \quad (4)$$

and

$$\Delta S_{\text{mix}} = -R \sum_i x_i \ln x_i \quad (5)$$

respectively, where H_{ij} is the enthalpy of mixing of the pair of the elements i and j at the equimolar concentration in binary systems, x_i and x_j are the atomic fraction of the elements i and j , respectively, and R is the gas constant.

The VEC is calculated from a rule of mixture as follows

$$\text{VEC} = \sum_i x_i \text{VEC}_i \quad (6)$$

where VEC_i is the VEC of the i -th element. Guo et al.^[27] demonstrated that VEC plays a relevant role for the prediction of the phase formation. Indeed, it can be seen as the physical parameter that controls the phase stability for BCC and FCC SSs. They showed that for $\text{VEC} < 6.87$, a BCC structure is prone to form, whereas for $\text{VEC} > 8$, FCC structure is more likely to occur. For intermediate VEC values, a mix of BCC and FCC phases is expected.

In 2008, Zhang and Zhou^[24] proposed for the first time a criterion based on δr and ΔH_{mix} to predict the stability of SSs, IM compounds, or bulk metallic glasses. According to their criterion, the formation of SSs is favored when the conditions $0.5\% < \delta r < 6.5\%$ and $-17.5 \text{ kJ mol}^{-1} < \Delta H_{\text{mix}} < 5 \text{ kJ mol}^{-1}$ are simultaneously valid.^[24] In 2013, Guo et al. achieved a similar result.^[65]

The plot of ΔH_{mix} as a function of δr for annealed RHEAs from the data of our database is shown in **Figure 1**. The data reported in the plot show a trend similar to that obtained by Zhang and Zhou.^[24] In the upper-left side of the plot there is

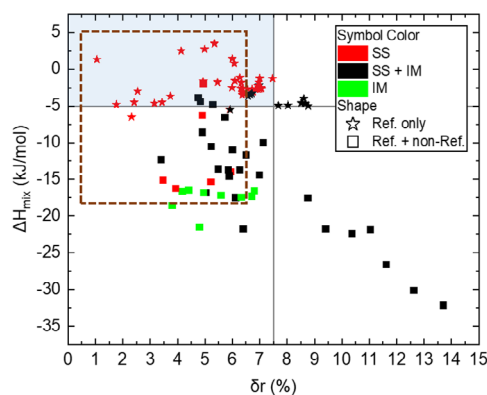


Figure 1. Plot of ΔH_{mix} as a function of δr for annealed RHEAs from the data collected in our database.

a region where alloys characterized by SSs are concentrated (red color), while, at the bottom and bottom-right boundaries the presence of IM compounds becomes predominant (black and green color). The field of SS stability proposed by Zhang and Zhou is delimited by the dashed box in **Figure 1**. However, it is evident that also numerous points that refer to RHEAs including IM phases are within that region. Moreover, it is possible to see that SSs are predominantly found in RHEAs based only on refractory elements, that is, Ti, V, Cr, Zr, Nb, Mo, Hf, Ta, W (star symbols), while IM compounds appear more prone to form in RHEAs containing also nonrefractory elements, such as Al and, in rarer cases, also C, Si, and Ni (square symbols).

In 2012, Yang and Zhang^[25] proposed a new criterion by introducing the Ω parameter, which is a descriptor that includes both entropic and enthalpic terms. Indeed, it is defined as

$$\Omega = \frac{T_m \Delta S_{\text{mix}}}{|\Delta H_{\text{mix}}|} \quad (7)$$

The plot of Ω as a function of δr for annealed RHEAs using the data included in the database that we developed is reported in **Figure 2**. It can be stated that the higher the value of Ω and the smaller the value of δr , the more the formation of SSs is favored. The ranges for having a stable SS, according to Yang and Zhang, are $\Omega \geq 1.1$ and $\delta r \leq 6.6\%$.^[25] This ranges define the region inside the dashed box in **Figure 2**. It is possible to notice that the proposed limit on Ω leads numerous RHEAs with IMs to be included in the proposed field of stability of SSs.

In 2014, Poletti and Battezzati^[26] proposed a criterion for the prediction of the stability of SSs and IM compounds based on the values of Allen electronegativity ($\delta\chi_A$). In 2016, Yurchenko et al. achieved similar results.^[66] More specifically, the Allen electronegativity is defined as the average ionization energy of the valence electrons for free atoms in their ground state.^[67,68] It is based on both experimental and theoretical values and shows values that are similar to Pauling electronegativity scale, but with a discrepancy for what concerns transition metal atoms. The plot of $\delta\chi_A$ as a function of δr for annealed RHEAs from the data of our database is shown in **Figure 3**. The field of stability of SSs can be found at low values of $\delta\chi_A$ and δr . The limits proposed by Poletti and Battezzati are $1\% < \delta r < 6\%$ and

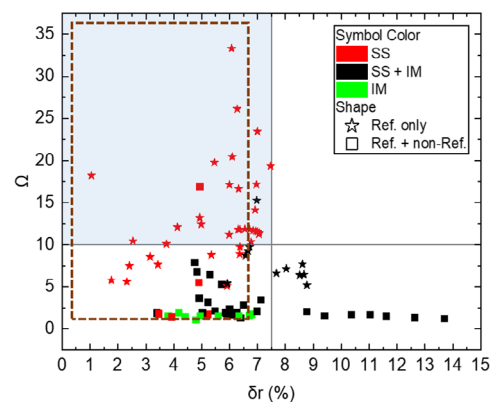


Figure 2. Plot of Ω as a function of δr for annealed RHEAs from the data collected in our database.

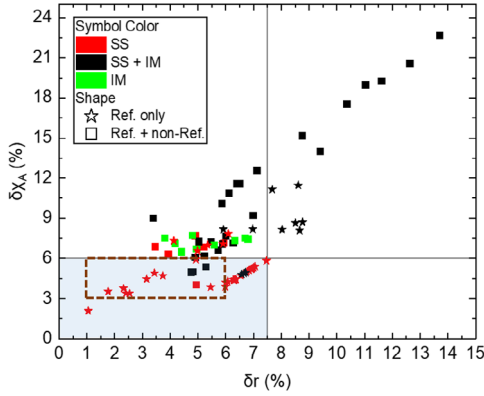


Figure 3. Plot of $\delta\chi_A$ as a function of δr for annealed RHEAs from the data collected in our database.

$3\% < \delta\chi_A < 6\%$.^[26] This region is delimited by the dashed box in Figure 3. We can notice that the proposed limits are valid, though quite conservative.

In 2015, Ye et al.,^[69] introduced the Φ parameter, given by the formula

$$\Phi(\xi) = \frac{\Delta S_{\text{mix}} - \Delta H_{\text{mix}}/T_{\text{m}}}{|S_{\text{XS}}(\xi)|} \quad (8)$$

where ξ is the packing factor, that is, 0.68 for BCC and 0.74 for FCC, and S_{XS} is the excess of configurational entropy that represents the deviation from the ideal SS. This thermodynamic variable was calculated through the Mansoori model.^[16,70,71]

$$S_{\text{XS}} = R[F_1(x_i, r_i, \xi) + F_2(x_i, r_i, \xi) + F_3(\xi)] \quad (9)$$

where

$$F_1(x_i, r_i, \xi) = -\frac{3}{2}(1 - \gamma_1 + \gamma_2 + \gamma_3) + (3\gamma_2 + 2\gamma_3)(1 - \xi)^{-1} + \frac{3}{2}\left(1 - \gamma_1 - \gamma_2 - \frac{1}{3}\gamma_3\right)(1 - \xi)^{-2} + (\gamma_3 - 1)\ln(1 - \xi) \quad (10)$$

$$F_2(x_i, r_i, \xi) = -\ln\{[(1 + \xi + \xi^2) - 3\xi(\gamma_1 + \gamma_2\xi) - \xi^3\gamma_3](1 - \xi)^{-3}\} \quad (11)$$

$$F_3(\xi) = -(3 - 2\xi)(1 - \xi)^{-2} + 3 + \ln[(1 + \xi + \xi^2 - \xi^3)(1 - \xi)^{-3}] \quad (12)$$

The terms γ_1 , γ_2 , and γ_3 can be calculated in the following way.

$$\gamma_1 = \sum_{j>i=1}^n \Delta_{ij}(d_i + d_j)(d_i d_j)^{-\frac{1}{2}} \quad (13)$$

$$\gamma_2 = \sum_{j>i=1}^n \Delta_{ij} \sum_{k=1}^n \left(\frac{\xi_i}{\xi}\right) \frac{(d_i d_j)^{\frac{1}{2}}}{d_k} \quad (14)$$

$$\gamma_3 = \left[\sum_{i=1}^n \left(\frac{\xi_i}{\xi}\right)^{\frac{2}{3}} x_i^{\frac{1}{3}} \right]^3 \quad (15)$$

where $d_i = 2r_i$ is the diameter of the i -th element and n is the number of constituent elements. The terms Δ_{ij} and ξ_i/ξ are calculated as in the following.

$$\Delta_{ij} = \left[\left(\frac{\xi_i}{\xi}\right)^{\frac{1}{2}} \left(\frac{\xi_j}{\xi}\right)^{\frac{1}{2}} \right] \left[\frac{(d_i - d_j)^2}{d_i d_j} \right] (x_i x_j)^{\frac{1}{2}} \quad (16)$$

$$\frac{\xi_i}{\xi} = \frac{d_i^3 x_i}{\sum_{k=1}^n (d_k^3 x_k)} \quad (17)$$

Since the Φ parameter depends on S_{XS} , it requires numerous operations to be calculated. However, from the plot reported in **Figure 4a**, it can be noted that the Φ parameter has an almost linear dependence with the Λ parameter, which was proposed in 2014 by Singh et al.^[72] It was defined as follows.

$$\Lambda = \frac{\Delta S_{\text{mix}}}{\delta r^2} \quad (18)$$

where δr^2 represents the elastic energy associated with lattice distortion with respect to a perfect lattice. Since Λ is directly proportional to ΔS_{mix} and inversely proportional to δr^2 , it is possible to make a comparison with Equation (8), which defines the Φ parameter. Due to the high melting temperatures of RHEAs,

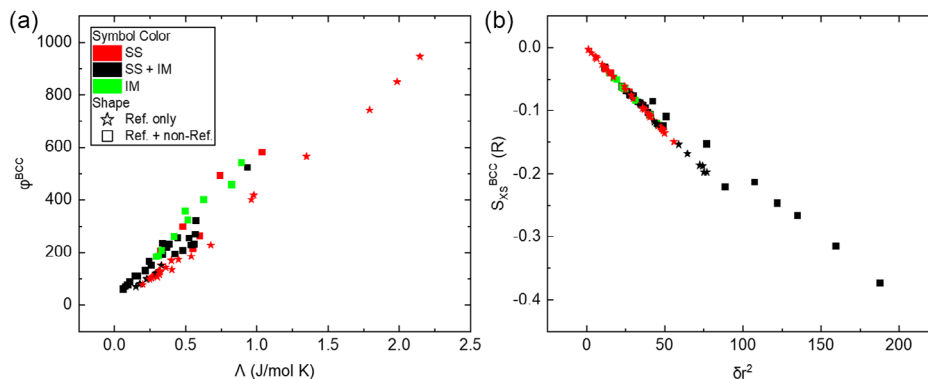


Figure 4. Plot of a) Φ as a function of Λ and b) S_{XS} as a function of δr^2 for annealed RHEAs from the data collected in our database.

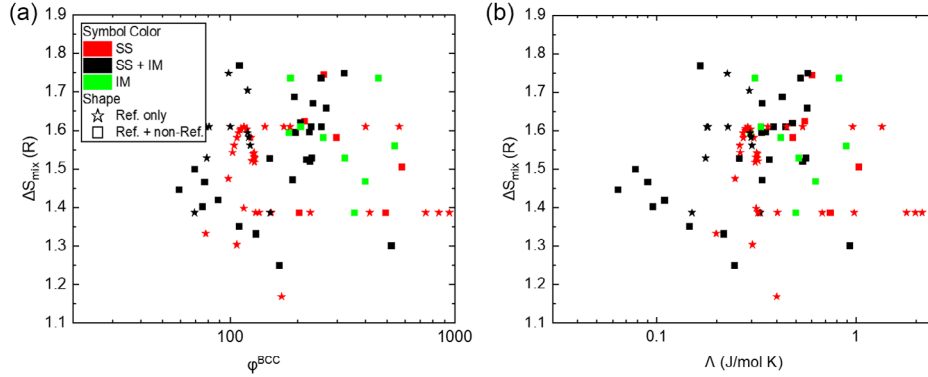


Figure 5. Plot of ΔS_{mix} as a function of a) Φ and b) Λ for annealed RHEAs from the data collected in our database.

the term $\Delta H_{\text{mix}}/T_m$ gives a small contribution to Φ . Thus, it is possible to consider $\Delta H_{\text{mix}}/T_m \approx 0$. Furthermore, as shown in Figure 4b, a near-linear dependence is found by plotting S_{XS} as a function of δr^2 , which is in agreement with the results of Takeuchi et al.^[73] Thus, it is possible to consider $S_{\text{XS}} \approx \delta r^2$. The conclusion is that the Φ parameter, which requires laborious calculations, could be replaced by the Λ parameter, which is easier to be determined. This is confirmed by the diagrams reported in **Figure 5**, where ΔS_{mix} is plotted as a function of Φ and Λ , respectively, showing a similar trend between ΔS_{mix} and the other two parameters.

Considering a dataset of about 50 HEAs, mainly FCC and FCC + BCC alloys, Ye et al.^[69] noticed that for $\Phi \geq 20$, single SSs were stable, while for $\Phi < 20$, multiple SSs and IMs were favorable. Therefore, the guideline proposed by Ye et al. to design HEAs consisted of maximizing Φ by increasing ΔS_{mix} and decreasing ΔH_{mix} and $|S_{\text{XS}}(\xi)|$.^[69,71] However, the criterion developed by Ye et al. does not apply to BCC RHEAs, as can be noticed from the plot of ΔS_{mix} as a function of Φ reported in Figure 5a. In this case, indeed, it is not possible to identify a unique region containing only SSs for $\Phi > 20$. This can be related to the fact that the dataset used by Ye et al. is based mainly on FCC HEAs. Therefore, their criterion can still be useful in the field of 3d transition metal HEAs.

In 2015, Troparevsky et al.^[74] proposed a thermodynamic criterion to determine the formation of SS phases in HEAs. They focused on the comparison between the Gibbs free energy of mixing (ΔG_{mix}) for SSs and the Gibbs free energy of formation of IM compounds (ΔG_{IM}). Since the enthalpic term in ΔG_{mix} and the entropic term in ΔG_{IM} are usually small, they assumed that they can be neglected and made use of the expressions

$$\Delta G_{\text{mix}} \approx -T_{\text{ann}} \Delta S_{\text{mix}} \quad (19)$$

and

$$\Delta G_{\text{IM}} \approx \Delta H_{\text{f}}^{\text{IM}} \quad (20)$$

where T_{ann} is the annealing temperature and the term $\Delta H_{\text{f}}^{\text{IM}}$ represents the most negative value of enthalpy of formation of binary IM phases between all the possible i and j pairs of alloying elements. According to Troparevsky et al., SS alloys are expected to have small values of $\Delta H_{\text{f}}^{\text{IM}}$.^[74]

In 2016, Senkov and Miracle^[75] proposed an enhanced version of the criterion of Troparevsky et al. by minimizing ΔG_{mix} with respect to ΔG_{IM} , that is

$$\Delta G_{\text{mix}} < \Delta G_{\text{IM}} \quad (21)$$

They obtained a condition for SS stability given by^[75]

$$\kappa_1 < \kappa_1^{\text{cr}}(T_{\text{ann}}) \quad (22)$$

where

$$\kappa_1 = \frac{\Delta H_{\text{IM}}}{\Delta H_{\text{mix}}} \quad (23)$$

and

$$\kappa_1^{\text{cr}}(T_{\text{ann}}) = -\frac{T_{\text{ann}} \Delta S_{\text{mix}}}{\Delta H_{\text{mix}}} (1 - k_2) + 1 \quad (24)$$

in which ΔH_{IM} was calculated from values of formation enthalpies for binary IMs^[74] through the formula

$$\Delta H_{\text{IM}} = \sum_{j \neq i}^n \sum_{i=1}^n 4 \Delta H_{ij}^{\text{IM}} x_i x_j \quad (25)$$

and the term $\kappa_2 = \Delta S_{\text{IM}}/\Delta S_{\text{mix}}$ was set equal to 0.6, as in the case of a partially ordered IM phase.^[2]

Senkov and Miracle validated their criterion with 45 annealed FCC and BCC HEAs. A plot of $\kappa_1^{\text{cr}}(T_{\text{ann}})$ as a function of κ_1 is reported in **Figure 6** for the annealed RHEAs that are listed in our database. As stated in Equation (22), a HEA should be in a SS state if it is located above the bisectrix of the plot, that is, in the region highlighted by the light blue shade in Figure 6. However, numerous SS RHEAs are also located slightly below the bisectrix. This may indicate that the fulfillment of the condition on κ_1 in Equation (22) cannot be considered as a unique guiding line to assess SS stability. Moreover, for $\kappa_1 < 2$, a consistent number of RHEAs above the bisectrix shows the presence of IMs. This can further limit the application of κ_1 as a prediction parameter for RHEAs.

In 2016, Sheikh et al.^[28] proposed for the first time a criterion which correlates the VEC and the room-temperature ductility. They stated that RHEAs with low VEC values are prone to exhibit

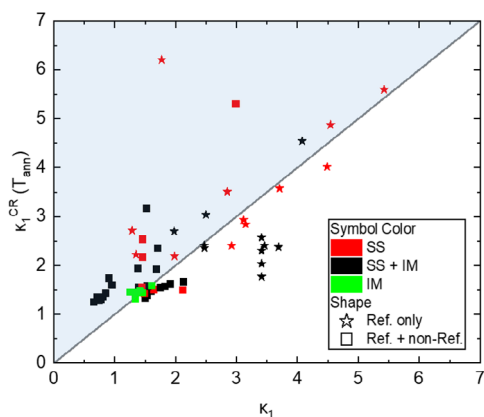


Figure 6. Plot of $\kappa_1^{CR}(T_{ann})$ as a function of κ_1 for annealed RHEAs from the data collected in our database.

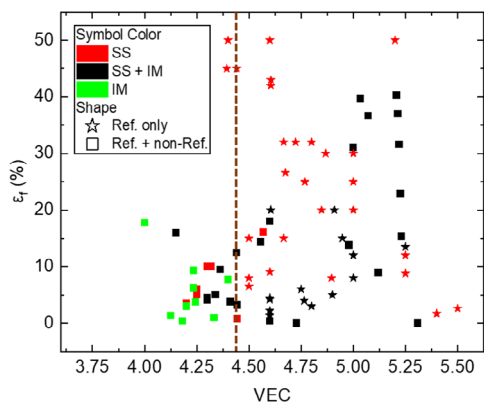


Figure 7. Plot of room-temperature compressive ε_f as a function of VEC for annealed RHEAs from the data collected in our database.

pronounced ductility. More precisely, when $VEC \leq 4.4$, it is more likely that RHEAs show marked ductility, while when $VEC \geq 4.6$ it is more likely that RHEAs show poor ductility. However, Sheikh et al. based their observations on nine RHEAs; therefore, it is important to validate this criterion with

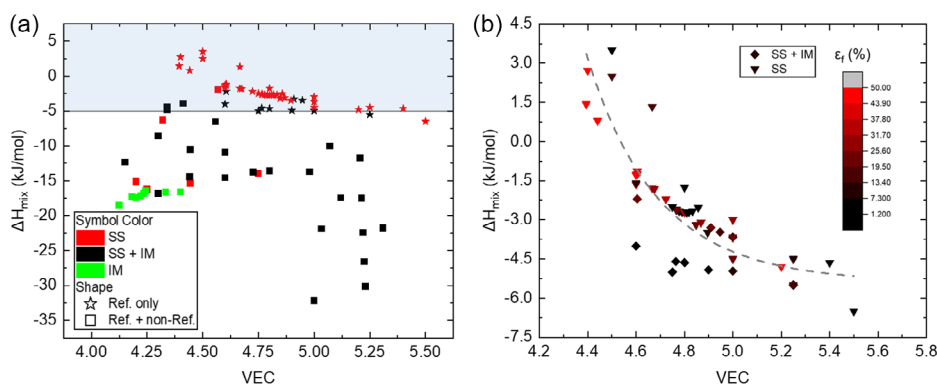


Figure 8. a) Plot of ΔH_{mix} as a function of VEC for annealed RHEAs from the data collected in our database. b) A portion of the previous plot for $\Delta H_{mix} > -7.5 \text{ kJ mol}^{-1}$.

a richer dataset. Moreover, a few years later, Senkov et al.^[76] pointed out that not a so clear brittle-to-ductile transition can be observed with the decrease of VEC in RHEAs.

In **Figure 7**, the room-temperature strain at fracture (ε_f) in compression is plotted as a function of the VEC for annealed RHEAs. The vertical dashed line highlights the value $VEC = 4.4$ below which, according to Sheikh et al., ductile RHEAs should be located.^[28] However, according to our data, for $VEC < 4.5$ the values of ε_f drop significantly. This can be related to the fact that almost all the alloys within this VEC range are characterized by the presence of IM compounds.

The plot in **Figure 8a** reports ΔH_{mix} as a function of VEC for the annealed alloys in our database, while **Figure 8b** reports the same data limited to the alloys whose composition spans on refractory elements only, that is, Ti, V, Cr, Zr, Nb, Mo, Hf, Ta, W. These alloys are mainly located in the shaded region in **Figure 8a**. From the graph reported in **Figure 8b**, it is possible to notice a nearly hyperbolic trend of ΔH_{mix} as a function of VEC for RHEAs based only on refractory elements. Combining these two parameters with the room temperature ε_f , the ductility tends to increase by decreasing the VEC and increasing the ΔH_{mix} . Such ductility is related to the stability of the SS phases, as shown by the plot in **Figure 8a**, where it is possible to observe that for high values of ΔH_{mix} , SSs tend to become the only stable phases.

4. New Criteria for Prediction of Solid Solution Stability and Final Remarks

As a concluding step of the present work, we propose new criteria based on the above results to design RHEAs characterized by stable SSs. All the possible correlations between pairs of Hume–Rothery and thermodynamic parameters of RHEAs in our database have been investigated. Considering only one parameter at a time, the determination of a region containing only SS alloys is not straightforward. A more reliable approach is to define threshold values based on a combination of at least two parameters.

Figure 9 and **10** show the relationships between couples of different parameters which have been considered in our analysis, in addition to those already shown in **Figure 1** to **3**. Vertical and horizontal threshold lines have been drawn to highlight the

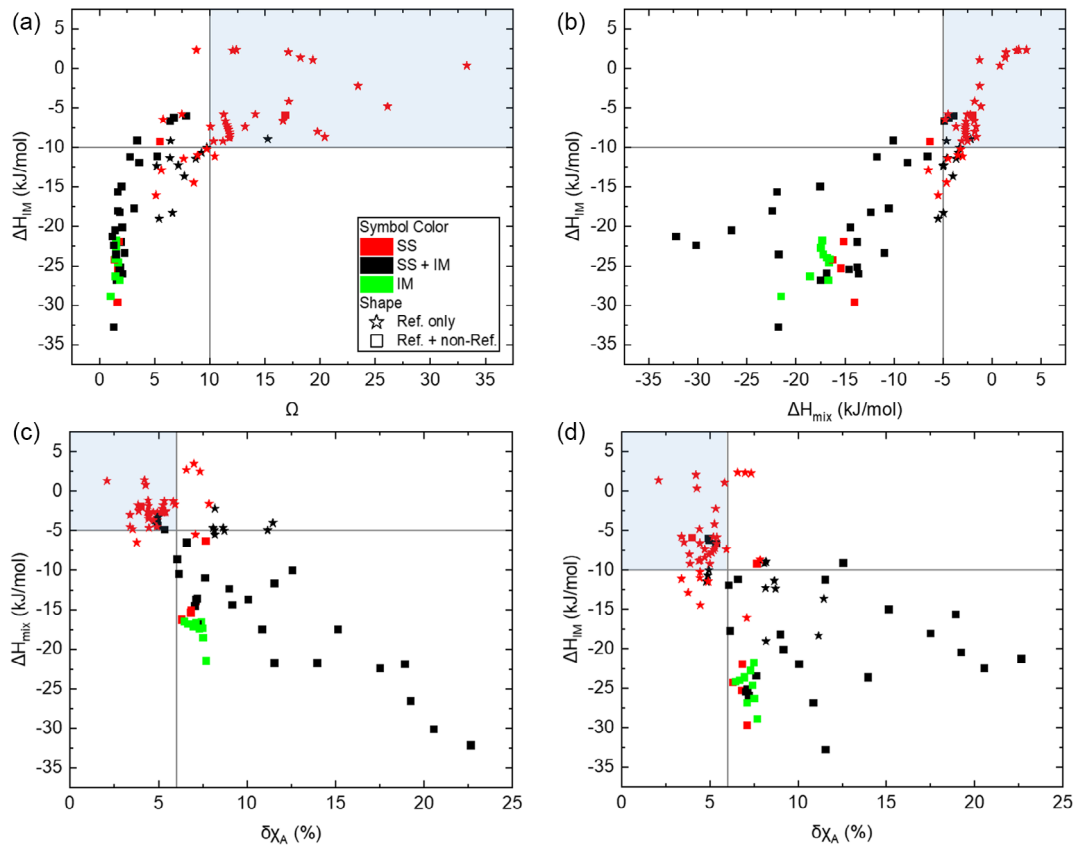


Figure 9. Plots showing the relationships between couples of different empirical parameters for annealed RHEAs from the data collected in our database. a) Plot of ΔH_{IM} as a function of Ω . b) Plot of ΔH_{IM} as a function of ΔH_{mix} . c) Plot of ΔH_{mix} as a function of $\delta\chi_A$. d) Plot of ΔH_{IM} as a function of $\delta\chi_A$.

proper boundary conditions for SS stability, and a shaded blue color has been used to further highlight the area characterized by the presence of SS RHEAs. Since a single parameter can be correlated with several other parameters, the threshold values for each parameter have been chosen in order to be valid for all the considered correlation diagrams (from Figure 1 to 3 and in Figure 9 and 10).

As shown in Figure 1, we propose to slightly change the limits defined by Zhang and Zhou^[24] in order to better fit the field of stability of SSs in the ΔH_{mix} - δr space. Indeed, more restrictive limits for ΔH_{mix} , that is, $-5 \text{ kJ mol}^{-1} < \Delta H_{mix} < 5 \text{ kJ mol}^{-1}$, seem to be more appropriate to exclude most of SS + IM data points. These limits work properly also in different parameter spaces, such as those shown in Figure 9b,c and 10c. Considering the relationship between Ω and δr —proposed by Yang and Zhang^[25] and reported in Figure 2—it seems more convenient to choose a higher limit for Ω according to our RHEA database. A proper value could be $\Omega > 10$, which is also in agreement with the data shown in Figure 9a and 10a. For what concerns $\delta\chi_A$, the limit $\delta\chi_A < 6\%$ proposed by Poletti and Battezzati^[26] appears to be appropriate also for RHEAs, as shown in Figure 3. This can also be confirmed by the graphs in Figure 9c,d and 10a,b. Another parameter which seems to work properly is ΔH_{IM} . Indeed, by the analysis of the data reported in Figure 9a,b,d and 10d, SSs appear to be stable within the range $-10 \text{ kJ mol}^{-1} < \Delta H_{IM} < 5 \text{ kJ mol}^{-1}$.

The threshold values proposed above appear to be able to divide the parameter spaces formed by coupling ΔH_{mix} , ΔH_{IM} , Ω and $\delta\chi_A$ into two major fields, that is, the field of stability of SSs and the field of formation of IMs. This is evident from the graphs in Figure 9 and 10a. On the other hand, when one of the abovementioned parameters is coupled with δr or VEC, the data appear to be more scattered. This can be seen in Figure 1, 2, and 3 for δr and in Figure 10b,c,d for VEC. Therefore, the threshold values for δr and VEC have been defined in order to extend as much as possible the field of SS stability when coupled with ΔH_{mix} , ΔH_{IM} , Ω , and $\delta\chi_A$. Our proposal is $\delta r < 7.5\%$ and $4.5 < \text{VEC} < 5.5$.

Thus, the full set of threshold values for all the different empirical parameters able to predict SS stability for RHEAs can be summarized as follows.

$$\delta r < 7.5\% \quad (26)$$

$$\Omega > 10 \quad (27)$$

$$\delta\chi_A < 6\% \quad (28)$$

$$4.5 < \text{VEC} < 5.5 \quad (29)$$

$$-5 \text{ kJ mol}^{-1} < \Delta H_{mix} < 5 \text{ kJ mol}^{-1} \quad (30)$$

$$-10 \text{ kJ mol}^{-1} < \Delta H_{IM} < 5 \text{ kJ mol}^{-1} \quad (31)$$

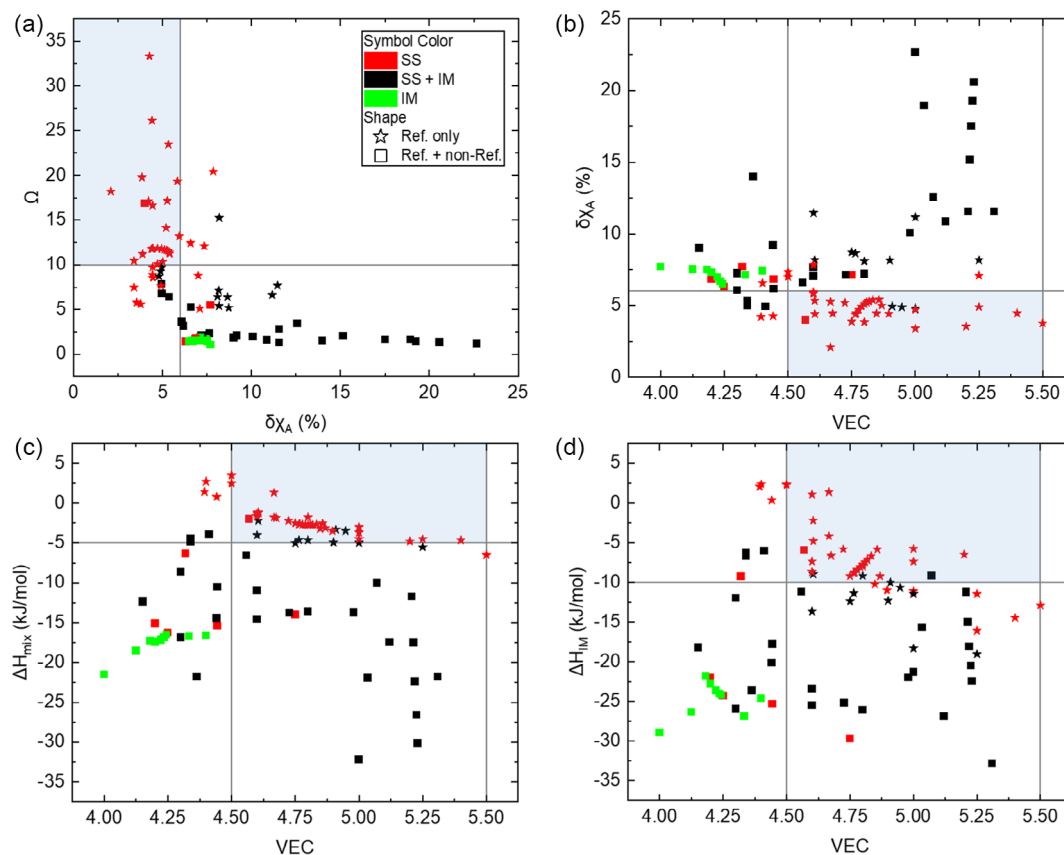


Figure 10. Plots showing the relationships between couples of different empirical parameters for annealed RHEAs from the data collected in our database. a) Plot of Ω as a function of $\delta\chi_A$. b) Plot of $\delta\chi_A$ as a function of VEC. c) Plot of ΔH_{mix} as a function of VEC. d) Plot of ΔH_{IM} as a function of VEC.

In conclusion, empirical criteria based on thermodynamic parameters have been shown to be able to profitably differentiate between SS RHEAs and RHEAs containing IM phases. Such kinds of models can be considered as a precious guideline for the high-throughput screening of unexplored RHEA compositions, thus reducing the experimental effort to design new high-performing refractory materials. However, the reliability of the predictive criteria is deeply chained to the quality of the associated datasets. Therefore, further investigation on a wider compositional range is required in order to confirm and/or improve the existing criteria. Finally, up to date, the criteria for the prediction of mechanical properties of RHEAs are very limited and mainly rely on alloys tested in compression. Therefore, more data on tensile tests of RHEAs are required in order to further improve reliability of current database.

Conflict of Interest

The authors declare no conflict of interest.

Data Availability Statement

The data that support the findings of this study are available from the corresponding author upon reasonable request.

Keywords

alloy designs, mechanical properties, phase stabilities, refractory high-entropy alloys, thermodynamic properties

Received: September 6, 2023

Revised: October 12, 2023

Published online:

- [1] E. P. George, D. Raabe, R. O. Ritchie, *Nat. Rev. Mater.* **2019**, *4*, 515.
- [2] D. B. Miracle, O. N. Senkov, *Acta Mater.* **2017**, *122*, 448.
- [3] Y. F. Ye, Q. Wang, J. Lu, C. T. Liu, Y. Yang, *Mater. Today* **2016**, *19*, 349.
- [4] J. W. Yeh, S. K. Chen, S. J. Lin, J. Y. Gan, T. S. Chin, T. T. Shun, C. H. Tsau, S. Y. Chang, *Adv. Eng. Mater.* **2004**, *6*, 299.
- [5] B. Cantor, I. T. H. Chang, P. Knight, A. J. B. Vincent, *Mater. Sci. Eng. A* **2004**, *375–377*, 213.
- [6] O. N. Senkov, D. B. Miracle, K. J. Chaput, J. P. Couzinie, *J. Mater. Res.* **2018**, *33*, 3092.
- [7] B. Gludovatz, A. Hohenwarter, D. Catoor, E. H. Chang, E. P. George, R. O. Ritchie, *Science* **2014**, *345*, 1153.
- [8] O. N. Senkov, G. B. Wilks, D. B. Miracle, C. P. Chuang, P. K. Liaw, *Intermetallics* **2010**, *18*, 1758.
- [9] O. N. Senkov, G. B. Wilks, J. M. Scott, D. B. Miracle, *Intermetallics* **2011**, *19*, 698.
- [10] Z. Li, K. G. Pradeep, Y. Deng, D. Raabe, C. C. Tasan, *Nature* **2016**, *534*, 227.

- [11] Y. Zhang, X. Yang, P. K. Liaw, *JOM* **2012**, *64*, 830.
- [12] X. Yang, Y. Zhang, P. K. Liaw, *Procedia Eng.* **2012**, *36*, 292.
- [13] O. N. Senkov, S. V. Senkova, C. Woodward, *Acta Mater.* **2014**, *68*, 214.
- [14] O. N. Senkov, C. Woodward, D. B. Miracle, *JOM* **2014**, *66*, 2030.
- [15] S. Guo, *Mater. Sci. Technol.* **2015**, *31*, 1223.
- [16] P. Martin, C. E. Madrid-Cortes, C. Cáceres, N. Araya, C. Aguilar, J. M. Cabrera, *Comput. Phys. Commun.* **2022**, *278*, 108398.
- [17] F. Zhang, C. Zhang, S. L. Chen, J. Zhu, W. S. Cao, U. R. Kattner, *CALPHAD: Comput. Coupling Phase Diagrams Thermochem.* **2014**, *45*, 1.
- [18] O. N. Senkov, J. D. Miller, D. B. Miracle, C. Woodward, *CALPHAD: Comput. Coupling Phase Diagrams Thermochem.* **2015**, *50*, 32.
- [19] F. Tian, *Front. Mater.* **2017**, *4*, 36.
- [20] A. Ferrari, B. Dutta, K. Gubaev, Y. Ikeda, P. Srinivasan, B. Grabowski, F. Körmann, *J. Appl. Phys.* **2020**, *128*, 150901.
- [21] Z. Rao, P. Y. Tung, R. Xie, Y. Wei, H. Zhang, A. Ferrari, T. P. C. Klaver, F. Körmann, P. T. Sukumar, A. K. da Silva, Y. Chen, Z. Li, D. Ponge, J. Neugebauer, O. Gutfleisch, S. Bauer, D. Raabe, *Science* **2022**, *378*, 78.
- [22] Z. Pei, J. Yin, P. K. Liaw, D. Raabe, *Nat. Commun.* **2023**, *14*, 1.
- [23] F. Otto, Y. Yang, H. Bei, E. P. George, *Acta Mater.* **2013**, *61*, 2628.
- [24] Y. Zhang, Y. J. Zhou, J. P. Lin, G. L. Chen, P. K. Liaw, *Adv. Eng. Mater.* **2008**, *10*, 534.
- [25] X. Yang, Y. Zhang, *Mater. Chem. Phys.* **2012**, *132*, 233.
- [26] M. G. Poletti, L. Battezzati, *Acta Mater.* **2014**, *75*, 297.
- [27] S. Guo, C. Ng, J. Lu, C. T. Liu, *J. Appl. Phys.* **2011**, *109*, 103505.
- [28] S. Sheikh, S. Shafeie, Q. Hu, J. Ahlström, C. Persson, J. Veselý, J. Zýka, U. Klement, S. Guo, *J. Appl. Phys.* **2016**, *120*, 164902.
- [29] C. Lee, G. Song, M. C. Gao, R. Feng, P. Chen, J. Brechtel, Y. Chen, K. An, W. Guo, J. D. Poplawsky, S. Li, A. T. Samaei, W. Chen, A. Hu, H. Choo, P. K. Liaw, *Acta Mater.* **2018**, *160*, 158.
- [30] Z. Wang, H. Wu, Y. Wu, H. Huang, X. Zhu, Y. Zhang, H. Zhu, X. Yuan, Q. Chen, S. Wang, X. Liu, H. Wang, S. Jiang, M. J. Kim, Z. Lu, *Mater. Today* **2022**, *54*, 83.
- [31] N. Yurchenko, E. Panina, M. Tikhonovsky, G. Salishchev, S. Zharebtsov, N. Stepanov, *Int. J. Refract. Met. Hard Mater.* **2020**, *92*, 105322.
- [32] Y. Guo, J. He, Z. Li, L. Jia, X. Wu, C. Liu, *Mater. Sci. Eng. A* **2022**, *832*, 142480.
- [33] O. Senkov, D. Isheim, D. Seidman, A. Pilchak, *Entropy* **2016**, *18*, 102.
- [34] O. N. Senkov, J. K. Jensen, A. L. Pilchak, D. B. Miracle, H. L. Fraser, *Mater. Des.* **2018**, *139*, 498.
- [35] Y. Guo, J. He, W. Lu, L. Jia, Z. Li, *Mater. Charact.* **2021**, *172*, 110836.
- [36] N. D. Stepanov, D. G. Shaysultanov, G. A. Salishchev, M. A. Tikhonovsky, *Mater. Lett.* **2015**, *142*, 153.
- [37] N. Y. Yurchenko, N. D. Stepanov, S. V. Zharebtsov, M. A. Tikhonovsky, G. A. Salishchev, *Mater. Sci. Eng. A* **2017**, *704*, 82.
- [38] N. Yurchenko, E. Panina, A. Belyakov, G. Salishchev, S. Zharebtsov, N. Stepanov, *Mater. Lett.* **2022**, *311*, 131584.
- [39] W. Chen, Q. H. Tang, H. Wang, Y. C. Xie, X. H. Yan, P. Q. Dai, *Mater. Sci. Technol.* **2018**, *34*, 1309.
- [40] S. Wu, D. Qiao, H. Zhang, J. Miao, H. Zhao, J. Wang, Y. Lu, T. Wang, T. Li, *J. Mater. Sci. Technol.* **2022**, *97*, 229.
- [41] S. Wu, D. Qiao, H. Zhao, J. Wang, Y. Lu, *J. Alloys Compd.* **2021**, *889*, 161800.
- [42] J. Yi, L. Wang, M. Xu, L. Yang, *Mater. Tehnol.* **2021**, *55*, 305.
- [43] X. J. Gao, L. Wang, N. N. Guo, L. S. Luo, G. M. Zhu, C. C. Shi, Y. Q. Su, J. J. Guo, *Int. J. Refract. Met. Hard Mater.* **2021**, *95*, 105405.
- [44] J. J. Yi, L. Wang, L. Yang, M. Q. Xu, *Phys. Met. Metallogr.* **2021**, *122*, 1500.
- [45] É. Fazakas, V. Zadorozhnyy, L. K. Varga, A. Inoue, D. V. Louzguine-Luzgin, F. Tian, L. Vitos, *Int. J. Refract. Met. Hard Mater.* **2014**, *47*, 131.
- [46] O. N. Senkov, C. F. Woodward, *Mater. Sci. Eng. A* **2011**, *529*, 311.
- [47] F. G. Coury, M. Kaufman, A. J. Clarke, *Acta Mater.* **2019**, *175*, 66.
- [48] J. Yi, L. Yang, L. Wang, M. Xu, *Met. Mater. Int.* **2022**, *28*, 448.
- [49] O. N. Senkov, S. V. Senkova, D. B. Miracle, C. Woodward, *Mater. Sci. Eng. A* **2013**, *565*, 51.
- [50] N. N. Guo, L. Wang, L. S. Luo, X. Z. Li, Y. Q. Su, J. J. Guo, H. Z. Fu, *Mater. Des.* **2015**, *81*, 87.
- [51] Y. Zhang, Y. Liu, Y. X. Li, X. Chen, H. W. Zhang, *Mater. Sci. Forum* **2016**, *849*, 76.
- [52] O. N. Senkov, J. M. Scott, S. V. Senkova, D. B. Miracle, C. F. Woodward, *J. Alloys Compd.* **2011**, *509*, 6043.
- [53] S. Maiti, W. Steurer, *Acta Mater.* **2016**, *106*, 87.
- [54] M. Todai, T. Nagase, T. Hori, A. Matsugaki, A. Sekita, T. Nakano, *Scr. Mater.* **2017**, *129*, 65.
- [55] Y. D. Wu, Y. H. Cai, X. H. Chen, T. Wang, J. J. Si, L. Wang, Y. D. Wang, X. D. Hui, *Mater. Des.* **2015**, *83*, 651.
- [56] H. W. Yao, J. W. Qiao, M. C. Gao, J. A. Hawk, S. G. Ma, H. F. Zhou, Y. Zhang, *Mater. Sci. Eng. A* **2016**, *674*, 203.
- [57] H. Chen, A. Kauffmann, B. Gorr, D. Schliephake, C. Seemüller, J. N. Wagner, H.-J. Christ, M. Heilmaier, *J. Alloys Compd.* **2016**, *661*, 206.
- [58] H. Chen, A. Kauffmann, S. Laube, I.-C. Choi, R. Schwaiger, Y. Huang, K. Lichtenberg, F. Müller, B. Gorr, H.-J. Christ, M. Heilmaier, *Metall. Mater. Trans. A* **2018**, *49*, 772.
- [59] E. S. Panina, N. Y. Yurchenko, S. V. Zharebtsov, M. A. Tikhonovsky, M. V. Mishunin, N. D. Stepanov, *Mater. Sci. Eng. A* **2020**, *786*, 139409.
- [60] N. D. Stepanov, N. Y. Yurchenko, D. V. Skibin, M. A. Tikhonovsky, G. A. Salishchev, *J. Alloys Compd.* **2015**, *652*, 266.
- [61] N. D. Stepanov, N. Y. Yurchenko, E. S. Panina, M. A. Tikhonovsky, S. V. Zharebtsov, *Mater. Lett.* **2017**, *188*, 162.
- [62] N. Yurchenko, E. Panina, M. Tikhonovsky, G. Salishchev, S. Zharebtsov, N. Stepanov, *Mater. Lett.* **2020**, *264*, 127372.
- [63] Z. P. Lu, H. Wang, M. W. Chen, I. Baker, J. W. Yeh, C. T. Liu, T. G. Nieh, *Intermetallics* **2015**, *66*, 67.
- [64] Z. Wang, Y. Huang, Y. Yang, J. Wang, C. T. Liu, *Scr. Mater.* **2015**, *94*, 28.
- [65] S. Guo, Q. Hu, C. Ng, C. T. Liu, *Intermetallics* **2013**, *41*, 96.
- [66] N. Yurchenko, N. Stepanov, G. Salishchev, *Mater. Sci. Technol.* **2017**, *33*, 17.
- [67] J. B. Mann, T. L. Meek, L. C. Allen, *J. Am. Chem. Soc.* **2000**, *122*, 2780.
- [68] J. B. Mann, T. L. Meek, E. T. Knight, J. F. Capitani, L. C. Allen, *J. Am. Chem. Soc.* **2000**, *122*, 5132.
- [69] Y. F. Ye, Q. Wang, J. Lu, C. T. Liu, Y. Yang, *Scr. Mater.* **2015**, *104*, 53.
- [70] G. A. Mansoori, N. F. Carnahan, K. E. Starling, T. W. Leland, *J. Chem. Phys.* **1971**, *54*, 1523.
- [71] Y. F. Ye, Q. Wang, J. Lu, C. T. Liu, Y. Yang, *Intermetallics* **2015**, *59*, 75.
- [72] A. K. Singh, N. Kumar, A. Dwivedi, A. Subramaniam, *Intermetallics* **2014**, *53*, 112.
- [73] A. Takeuchi, K. Amiya, T. Wada, K. Yubuta, W. Zhang, A. Makino, *Entropy* **2013**, *15*, 3810.
- [74] M. C. Tropicovsky, J. R. Morris, P. R. C. Kent, A. R. Lupini, G. M. Stocks, *Phys. Rev. X* **2015**, *5*, 011041.
- [75] O. N. Senkov, D. B. Miracle, *J. Alloys Compd.* **2016**, *658*, 603.
- [76] O. N. Senkov, D. B. Miracle, S. I. Rao, *Mater. Sci. Eng. A* **2021**, *820*, 141512.